Pittsburgh Interdisciplinary Mathematics Review **4** (2026), 18–55

Optimal packings of coins and oranges

Daria Pchelina

(Communicated by Lark Song
Copyedited by Sophie Li and Lucas Pasdo)

Abstract

The field of optimal packings belongs to the realm of "intuitive geometry" — a term introduced by László Fejes Tóth to describe geometry problems that are easy to state but extremely difficult to solve. Today, "difficult" often implies the need for computer assistance, as illustrated by the proofs of the Kepler conjecture and the four-color theorem. Such problems lie at the interface of the continuous and the discrete: to solve them, one must combine analytical (continuous) methods and computer calculations (discrete). A solid theoretical foundation is needed to make the computations feasible in terms of time and memory. The proofs of the Kepler conjecture and of the four-color theorem were eventually verified by computer, which is natural given that proofs of this magnitude are impossible to fully check by hand, and their significance made formal confirmation essential to the community. This inseparable triplet of *complicated conjecture*, *computer assistance*, and eventual *formal verification* will undoubtedly appear again in future results. In this article, we explore optimal disk and sphere packings, a domain that originated with the Kepler conjecture, where geometry and computation interact in various surprising ways.

Contents

1. From coins to oranges and beyond

How should we place one-euro coins (i.e., congruent disks) on a table (two-dimensional space) without overlap to cover as much surface as possible? After a brief reflection, the reader probably imagined one of the arrangements in Figure 1. The left-hand arrangement covers about 78% of the plane, while the right-hand one, called the *hexagonal packing*, covers more than 90%. This pattern, *optimal* in terms of coin packing, has been used by bees since long before humans started to play with coins (Figure 2).

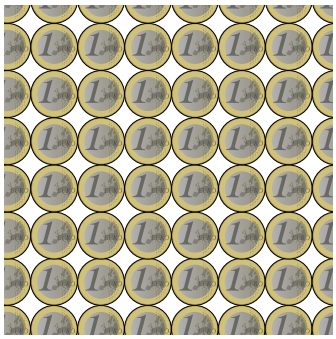

Figure 1: Two ways to arrange one-euro coins.

Figure 2: A honeycomb.[1]

[1]Matthew T Rader, MatthewTRader.com, License CC-BY-SA

Consider the analogous question in three dimensions: *What is the densest way to stack oranges?* It turns out that the optimal packing is the one we see on market stalls, as the one in Figure 3. It is constructed by superposing layers of spheres centered on square grid, as shown in Figure 4, on the left. Viewed from the side, we obtain the triangles of spheres from a hexagonal arrangement, depicted on the right in Figure 4. In 1611, Kepler conjectured that this was the optimal way to pack cannonballs [Kep11]. Remarkably, this conjecture was resolved only 400 years later by a long computer-assisted proof [HF06]. We will come back to the Kepler conjecture in Section 4.1.

Figure 3: Oranges at the market.[2]

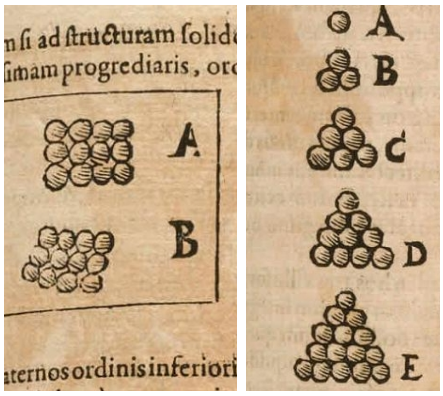

Figure 4: Illustrations by Kepler [Kep11].

Those whose imagination is not confined to the physical world study optimal sphere packings in higher dimensions. These problems have applications in information theory, particularly in the construction of error-correcting codes. Thanks to Viazovska's breakthroughs, the sphere packing problem is now solved in dimensions 8 and 24 [Via17, CKM+17]. She received the Fields Medal in 2022 for these contributions.

Another generalization of the coin arrangement problem is to use coins of two different sizes. For example, the best way to cover a table with the two coins

is shown in the middle of Figure 5. The solution depends on the ratio between the coin sizes. The arrangements on the left and on the right in Figure 5 are optimal for the corresponding ratios. In Section 3 we will discuss these results and also examine other optimal arrangements with two and three coin sizes.

[2] https://www.reddit.com/r/oddlysatisfying/comments/b75dgf/this_display_of_oranges/

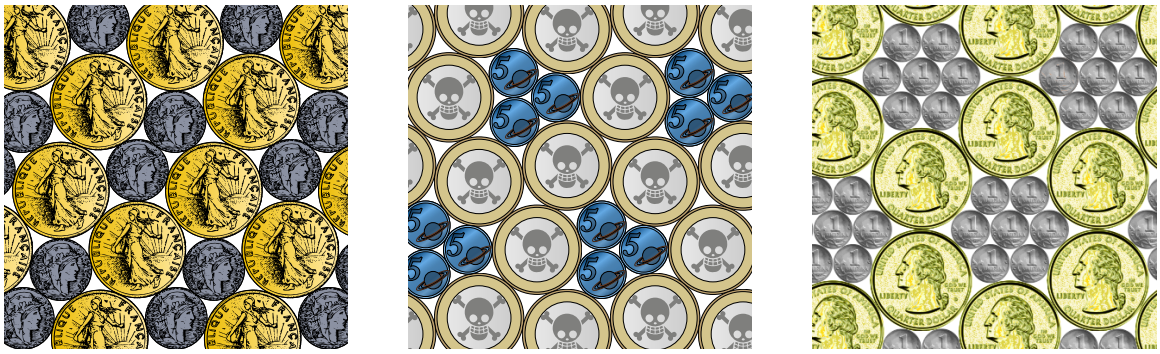

Figure 5: Optimal arrangements for each pair of coin sizes.

Let us increase both the dimension of the space and the number of sphere sizes. For example, consider the packing of oranges and cherries shown in Figure 6: each cherry has exactly the right size to fit into the hole formed by an octahedron of six oranges. This packing reproduces the configuration of sodium ions (cherries) and chloride ions (oranges) in the crystalline structure of sodium chloride — the main component of table salt. We will return to this "salt" packing in Section 4.

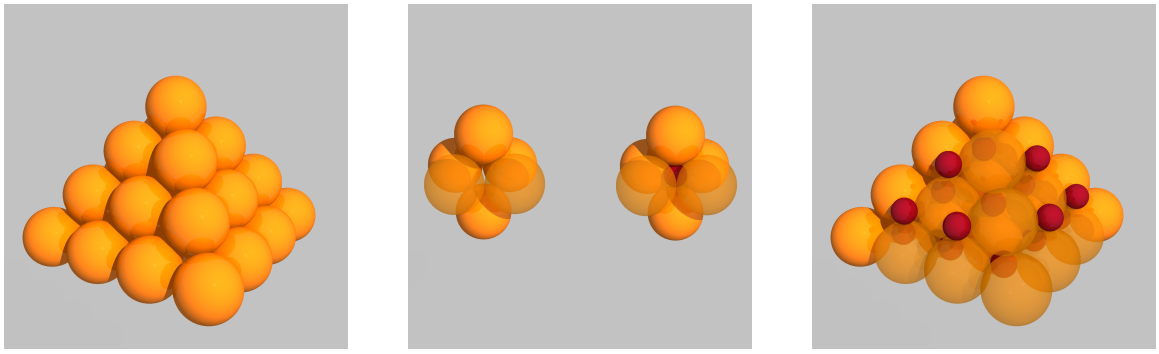

Figure 6: Inserting cherries in the optimal packing of oranges (left) to get the atomic structure of the salt crystals (right).

This observation naturally points toward an application of packing problems: chemists are interested in optimal disk and sphere arrangements because such configurations may help them to design compact materials using spherical nanoparticles of prescribed sizes [PDKM15, HST12]. In fact, the self-assembly of spherical and cylindrical nanoparticles often corresponds to optimal disk or sphere packings [CCMFT23]. Figure 7 illustrates experimental results from [PDKM15].

Another, more down-to-earth application of optimal packings is actually packing physical objects of realistic size — such as oranges in crates or cylindrical pipes in shipping containers. Up to this point, we have focused on infinite packings of the

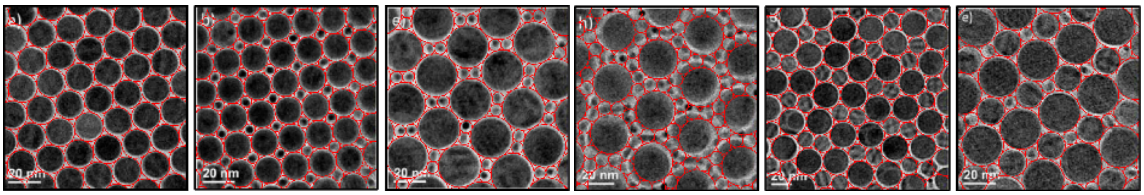

Figure 7: Arrangements self-assembled from colloidal nanodisks and nanorods in [PDKM15] precisely corresponding to optimal disk packings.

entire plane or of higher-dimensional spaces. In real life, objects must fit inside a bounded region, and the optimal arrangements in containers are often quite different from the optimal infinite packings. We begin our journey by studying finite disk packings in circular and square containers in Section 2.

2. **Disks in boxes**

Our main question is the following: given n identical disks, what is the smallest square (or circular) container in which they can be placed without overlap, and what are the corresponding optimal arrangements? A variety of methods are used to study this problem. Sometimes, we prefer to consider point arrangements instead of disk packings, while at some point, we will even replace disks by billiard balls!

2.1. **Points vs disks**

For the sake of simplicity, let us first consider the case of a circular container. We formally define the set of packings of n identical disks of radius r in a circle of radius R as follows.

$$P_n(r,R) := \{(b_1,\dots,b_n) \text{ such that } b_i \subseteq B(0,R) \text{ and } \operatorname{int}(b_i)\cap\operatorname{int}(b_j)=\emptyset \quad \forall i\neq j\},$$

where $B(0,R) := \{x\in\mathbb{R}^2 \,|\, |x|\leq R\}$ is the circular container of radius R centered in the origin and $b_1,\dots,b_n$ are disks of radius r with non-overlapping interiors (i.e., a pair of disks can be tangent but can not intersect).

Let us now introduce the first two formulations of our problem.

Problem 1. *Find the smallest circular container such that n unit disks fit inside,*

$$R_n := \min_{P_n(1,R)\neq\emptyset} R.$$

Problem 2. *Find the biggest r such that n disks of radius r fit into the unit circular container,*

$$r_n := \max_{P_n(r,1)\neq\emptyset} r.$$

They are equivalent: one can go from one to the other applying a simple homothety.

Lemma 2.1 (Problem 1∼Problem 2)**.** *P is an optimal packing of n unit disks, i.e. $P \in P_n(1, R_n)$, if and only if applying the $\frac{1}{R_n}$-homothety to P, we get an optimal n-disks packing in a unit circle, i.e., $\frac{1}{R_n} \cdot P \in P(r_n, 1)$, and $r_n = \frac{1}{R_n}$.*

We leave the proof of this lemma to the reader (see Figure 8 for illustration).

We define the set of *n-point arrangements* with pairwise distance at least d in a circle of radius R as follows:

$$A_n(d, R) := \{p_1, \dots, p_n \in \mathbb{R}^2 \text{ such that } p_i \in B(0, R) \text{ and } |p_i - p_j| \geq d \quad \forall i \neq j\}.$$

Now let us consider two formulations of the optimal point arrangements problem.

Problem 3. *Find the smallest circular container such that n points with pairwise distance at least 1 fit inside,*

$$R'_n := \min_{A_n(1,R') \neq \emptyset} R'.$$

Problem 4. *Find the biggest d such that n points with pairwise distance at least d fit inside the unit circular container,*

$$d_n := \max_{A_n(d,1) \neq \emptyset} d.$$

Problem 3 and Problem 4 are equivalent for the same reason as before: it is enough to apply an R'_n-deflation to a solution of Problem 3 to get a solution of Problem 4. Moreover, they both are also equivalent to the disk packing problems:

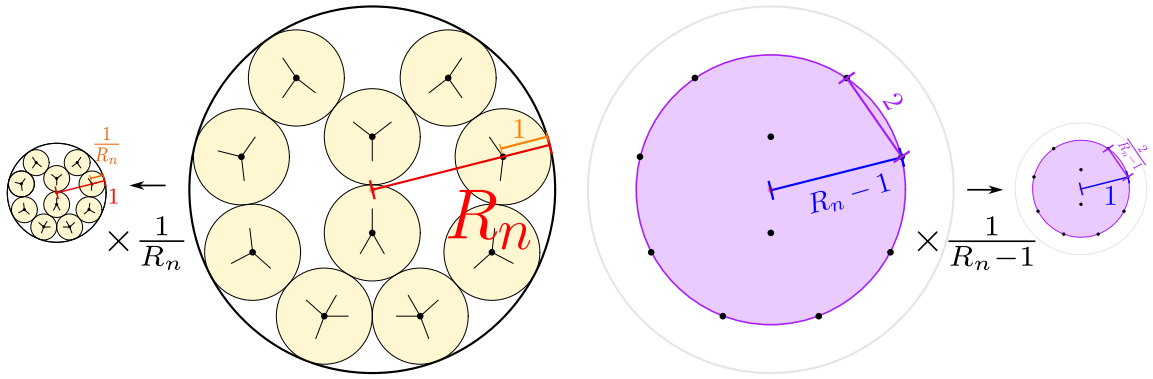

Figure 8: Illustration of the equivalence between Problems 1–4 for $n = 10$.

Lemma 2.2 (Problem 1∼Problem 4)**.** *If $P = \{b_i\}_{i=1}^n \in P_n(1, R_n)$ where $b_i = B(c_i, 1)$ then applying the $\frac{1}{R_n - 1}$ homothety to the centers of disks in P, we get an optimal n-points arrangement in a unit circle, i.e., $\{\frac{c_i}{R_n - 1}\}_{i=1}^n \in A(d_n, 1)$ and $d_n = \frac{2}{R_n - 1}$.*

We leave the proof of this lemma to the reader — once again, Figure 8 illustrates the transition.

In what follows, we will switch between the aforementioned formulations depending on the context. To go from one to another, it is enough to keep in mind the following relations between the optimal values:

$$r_n = \frac{1}{R_n}, \qquad d_n = \frac{2}{R_n - 1},$$

where r_n is the radius of disks in an optimal disk packing in the unit circle, R_n is the smallest radius of a circle containing n unit disks, and d_n is the maximal value of the minimal pairwise distance of n points in a unit circle.

In the same way, one can obtain the analogous relations for square containers (see Figure 9):

$$r_n = \frac{1}{S_n}, \qquad d_n = \frac{2}{S_n - 2}, \tag{$\square$}$$

where r_n is the radius of the disks in an optimal packing inside the unit square, S_n is the smallest side length of a square that can contain n unit disks, and d_n is the maximal value of the minimal pairwise distance among n points in the unit square.

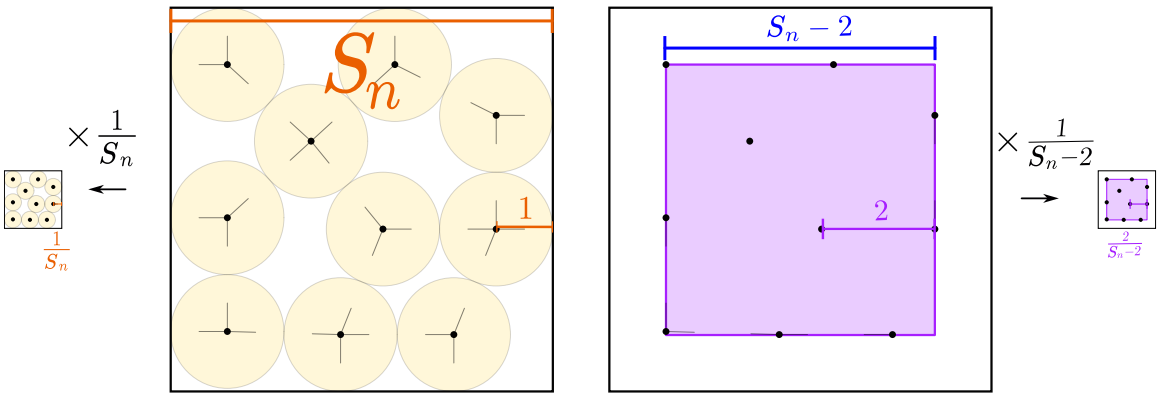

Figure 9: Illustration of the equivalence between different formulations for square containers for $n = 10$.

2.2. **Mathematical programming**

Let us briefly recall some basic notions from mathematical programming. In general, a mathematical programming problem is an optimization problem, where we aim to find the best (min or max) value of a certain quantity, called the *objective value*, subject to a set of constraints. A *feasible solution* is any choice of variables that satisfies all the constraints, and the *optimal solution* is a feasible solution that maximizes or minimizes the objective value, depending on the problem.

Our packing problems are indeed optimization problems. The most direct way to formulate them in terms of mathematical programming is to use the point-arrangement version, where we try to maximize the minimal pairwise distance among the points placed in a unit circle or square.

Let us introduce variables representing the coordinates of the points, together with an additional variable t representing the squared minimal pairwise distance, to get rid of the square root. Instead of using a min function, we impose a constraint for each pair of points, ensuring that t is no greater than the squared distance between the points. The optimal value d_n is then equal to the square root of the maximal objective value of this problem.

$$\begin{aligned}
&\text{Maximize } t \\
&\qquad \text{s.t. } t \le (x_i - x_j)^2 + (y_i - y_j)^2 \qquad \frac{n(n-1)}{2} \text{ non-convex constraints} \\
&\text{square container: } 0 \le x_i \le 1,\ 0 \le y_i \le 1 \qquad 2n \text{ linear constraints} \\
&\text{circular container: } 0 \le x_i^2 + y_i^2 \le 1 \qquad n \text{ convex constraints}
\end{aligned}$$

This is a quadratic, non-convex, inequality-constrained optimization problem. This kind of problem is too hard for analytical approach and even with computer assistance, using global optimization solvers, it is impossible to get solutions starting from $n = 6$ [SMC+07]. In other words, we should never forget about geometry!

Before trying to find optimal solutions of this problem let us first find bounds on the objective value.

2.3. **Lower bound on** d_n

A lower bound on the optimal objective value is given by the objective value of any feasible solution. Our goal is therefore to construct a feasible solution that is good enough to provide a meaningful lower bound. We begin by showing how to place at least $\frac{2s^2}{\sqrt{3}}$ points at pairwise distance at least 1 inside a square of side length s, for any $s \in \mathbb{R}^+$.

We divide the square into horizontal bands of height $\frac{\sqrt{3}}{2}$, starting from the bottom of the square (the topmost band may be narrower). These bands are delimited by the red segments in Figure 10. Let

$$N = \left\lfloor \frac{2s}{\sqrt{3}} \right\rfloor + 1$$

denote the number of red segments. Place $\lfloor s \rfloor + 1$ points on each odd segment, so that the first point is stuck to the left side of the square and each pair of neighbor points is at distance 1. Now place $\left\lfloor s - \frac{1}{2} \right\rfloor + 1$ points on each even segment, so that

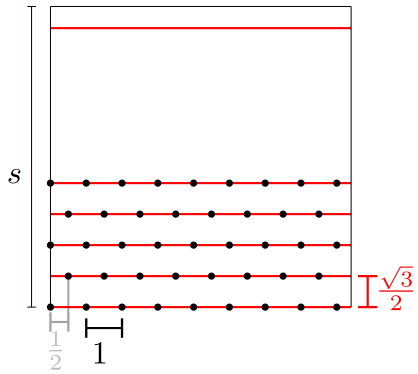

Figure 10: Placing at least $\frac{2s^2}{\sqrt{3}}$ points at distance at least 1 in a square of side s.

the first point is at offset $\frac{1}{2}$ from the left side of the square, and each pair of neighbors is still at distance 1. This way, the minimal pairwise distance of all points in the square equals 1.

The total number of points equals

$$\begin{cases} \frac{N}{2}\left(\lfloor s\rfloor + 1 + \lfloor s - \frac{1}{2}\rfloor + 1\right), & \text{if } N \text{ is even,} \\ \frac{N-1}{2}\left(\lfloor s\rfloor + 1 + \lfloor s - \frac{1}{2}\rfloor + 1\right) + \lfloor s\rfloor + 1, & \text{if } N \text{ is odd.} \end{cases}$$

In both cases, the total number of points is at least equal to

$$Ns \geq \frac{2s^2}{\sqrt{3}}.$$

Scaling by $d = \frac{1}{s}$, we obtain an arrangement of at least $\frac{2}{d^2\sqrt{3}}$ points at distance at least d in the unit square, for all $d \in \mathbb{R}^+$.

Finally, for any $n \in \mathbb{N}$, taking $d = \sqrt{\frac{2}{n\sqrt{3}}}$, we can place at least n points at distance at least $\sqrt{\frac{2}{n\sqrt{3}}}$ in the unit square.

Thus, we obtain the lower bound of the objective value:

$$d_n \geq \sqrt{\frac{2}{n\sqrt{3}}}.$$

2.4. **Upper bound on** r_n

To obtain an upper bound on the maximal pairwise distance, it is more convenient to return to the disk-packing point of view. The upper bound on d_n will be derived from an upper bound on the maximal disk radius r_n. To get this upper bound, we first cut packings into small pieces.

Given a set of points $S \subset \mathbb{R}^2$, the *Voronoi cell* $\mathrm{Vor}(p)$ of a point $p \in S$ is defined as the set points of the plane which are closer to p than to any other point from S. More formally,

$$\mathrm{Vor}(p) := \left\{ q \in \mathbb{R}^2 \;\middle|\; |p - q| \leq |p' - q| \; \forall p' \in S \setminus \{p\} \right\}.$$

A Voronoi cell is a convex, possibly unbounded, polygonal domain. The *Voronoi diagram* of S is the union of the Voronoi cells of its points.

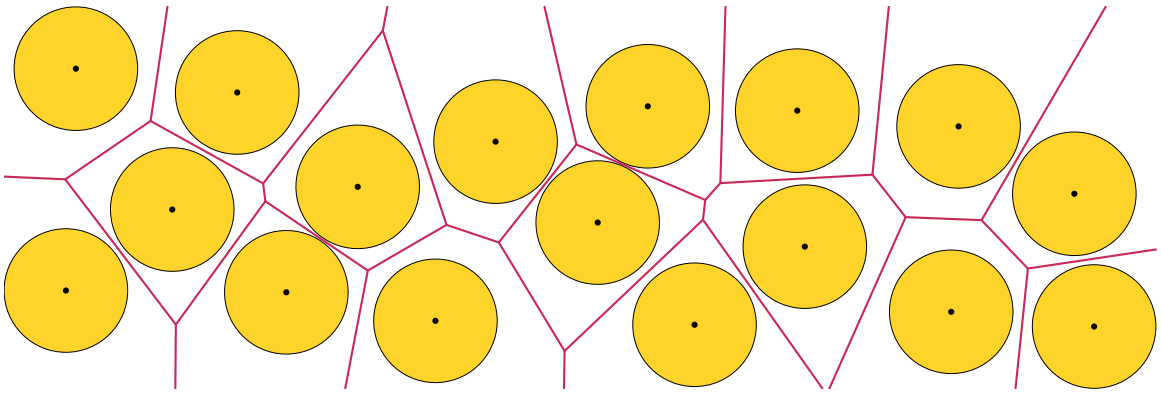

Figure 11: Voronoi diagram of a disk packing.

The Voronoi diagram of a disk packing is defined as the Voronoi diagram of the disk centers, as illustrated in Figure 11.

What is the Voronoi cell of the smallest area in a packing of unit disks?[3] First, we can restrict ourselves to circumscribed polygons: indeed, if one of the sides of the cell is not tangent to the disk, moving it closer to the disk only diminishes the area, as shown on the left of Figure 12.

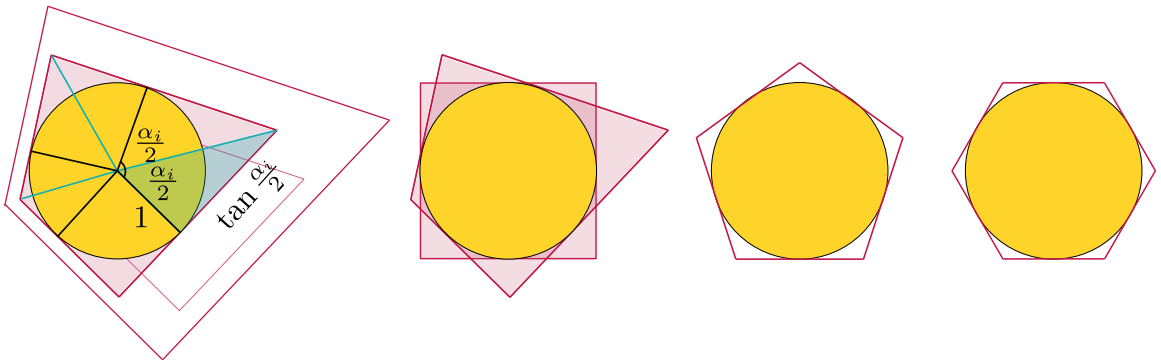

Figure 12: Illustration of minimizing the area of a Voronoi cell around a disk.

[3]Answered by Rogers who also obtained an upper bound in n-dimensional case [Rog58].

Our aim now is to find the circumscribed polygon of minimal area. The area of a k-gon circumscribed around a unit disk can be written as

$$\sum_{i=1}^{k} \tan\left(\frac{\alpha_i}{2}\right),$$

where α_i are the angles between consecutives prependiculars drawn from the disk center to the sides of the polygon (see the illustration on the left in Figure 12). Since $\tan\left(\frac{x}{2}\right)$ is a convex function and the angles α_i sum to 2π , we have

$$\frac{1}{k}\sum_{i=1}^{k} \tan\frac{\alpha_i}{2} \geq \tan\left(\frac{\sum_{i=1}^{k}\alpha_i}{2k}\right) = \tan\frac{\pi}{k}.$$

Therefore, the circumscribed polygon of minimal area must be regular. The regular hexagon is optimal among all regular circumscribed polygons with at most six sides. A Voronoi cell with seven or more edges must have some of its sides at a noticeably larger distance from the center, since at most six unit disks can touch a given unit disk; this forces its area to be significantly larger than that of the regular hexagon.[4] It follows that the Voronoi cell of the area in a packing of unit disks is a circumscribed regular hexagon.

Let us now consider a feasible solution of Problem 3, i.e., a packing of n disks of radius r in a unit square, as depicted in Figure 13. As shown above, the area of any Voronoi cell is at least the area of a regular hexagon circumscribed around a disk of radius r, which equals $2\sqrt{3}r^2$.

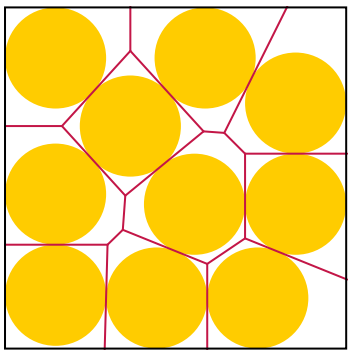

Figure 13: Voronoi diagram of a disk packing in a square.

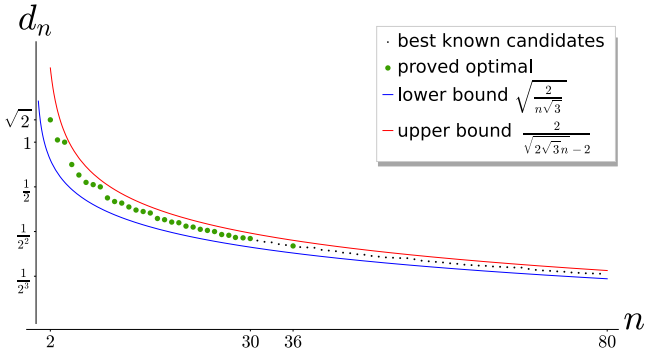

Figure 14: Lower and upper bounds on d_n. Points correspond to the best known arrangements; green points are those proved optimal.

[4]You will find a complete formal proof of this fact in [MSS22].

Since Voronoi cells are disjoint and their union is the unit square, we obtain

$$n \cdot 2\sqrt{3}r^2 \leq \sum_{i=1}^{n} \operatorname{area}(\operatorname{Vor}(c_i)) = 1.$$

This implies an upper bound on the disk radius r in any feasible packing, and, therefore, on maximal disk radius r_n. Using ($\square$), we also obtain the upper bound on d_n:

$$r_n \leq \sqrt{\frac{1}{2\sqrt{3}n}} \implies d_n = \frac{2}{\frac{1}{r_n} - 2} \leq \frac{2}{\sqrt{2\sqrt{3}n} - 2}.$$

Together, these bounds describe the behaviour of the optimal distance, shown in Figure 14.

2.5. **What is a solution?**

When studying packing problems, it is important to clarify what we mean by a "solution". At the most basic level, one may obtain a *numerical candidate packing*, produced for instance by hand at the blackboard, or by running a computer simulation based on some heuristic. Without taking precautions, such a candidate may not even be feasible (i.e., it may fail to form a valid packing) due to rounding errors, and its objective value is generally unreliable.

If we verify that the numerical candidate from before does indeed satisfy all constraints, we obtain a feasible arrangement that may or may not be optimal; we call this a *candidate packing*.

Beyond this, one may aim for an *enclosure of the optimum*, that is, a rigorously certified interval of packings guaranteed to contain the optimal ones. Ultimately, the goal is to obtain the set of *optimal packings*, feasible configurations that are mathematically proved to be globally optimal.

In what follows, the early stages cannot be skipped: each level is essential for reaching the next. We therefore begin by searching for numerical candidates, approximate packings that seem "good enough" and can serve as starting points for further refinement.

2.6. **Billiards in a box**

Several simulation approaches were developed to find good candidate configurations, and the best results are in fact obtained by combining multiple methods. Here we give just a few examples.

The *billiard simulation* method, introduced in 1990 [LS90], produced many "new" candidates at the time. One starts with n identical disks of a small initial radius and

random initial velocity vectors in a container. All disks then inflate simultaneously while undergoing elastic collisions; inflation stops once motion is no longer possible. This idea has remained at the core of the most effective techniques for producing candidate packings until today.

In the *modified billiard simulation* [SMC+07] (also known as the pulsating disk shaking algorithm), disks have no initial velocity prior to their first collision. Only local interactions (circle-circle or circle-wall contacts) are stored, which significally improves the speed of computations.

In the *point-based* method, we consider arrangements of points subject to repulsive forces. This approach was introduced in [BDGL00] yielding new arrangements in square containers up to $n = 200$. The algorithm proceeds as follows:

- Initialize n random points in the unit square; set $\varepsilon = \frac{1}{4}$.
- For each point, shift it by ε in one of four directions (left, up, right, down) in order to increase its distance to its nearest neighbor; do not move it otherwise. Repeat until no point is shifted.
- Reduce the step size: $\varepsilon \leftarrow \frac{2\varepsilon}{3}$.
- Stop once ε is sufficiently small.

This algorithm must be run many times from different initial configurations to produce good results.

To verify the feasibility of the numerical candidate obtained at the end of the simulation, one should use interval analysis. In *interval arithmetic*, numerical values (e.x., point coordinates) are replaced by intervals, and each arithmetic operation is performed so as to produce an interval guaranteed to contain all possible results. An inequality between two intervals is considered to hold only if the corresponding inequality is satisfied for every pair of values taken from the two intervals. Interval arithmetic is implemented for programming languages such as C, C++, SageMath, and Julia through dedicated numerical libraries, and is widely used in computational geometry to obtain certified results.[5]

Interval arithmetic allows us to replace each point of the arrangement by a small error-square and to check the constraints on all possible choices of points inside these squares at once. If interval analysis confirms that the error-squares entirely satisfy the constraints, then we obtain an enclosure of feasible arrangements. If some constraint is not verified, each square is subdivided into four smaller squares, and the test is

[5]To better understand why floating-point arithmetic fails when it comes to geometry, please see [KMP+08].

repeated on all combinations of smaller squares. This subdivision process can be continued as necessary.

2.7. **Proving optimality by hand**

For a small number of disks, optimal packings can be found (and their optimality proved) entirely by hand. In fact, for all optimal packings in a circular container, the existing proofs were obtained without the use of computers. Let us consider the cases up to $n = 7$. The optimal point arrangements are depicted in Figure 15.

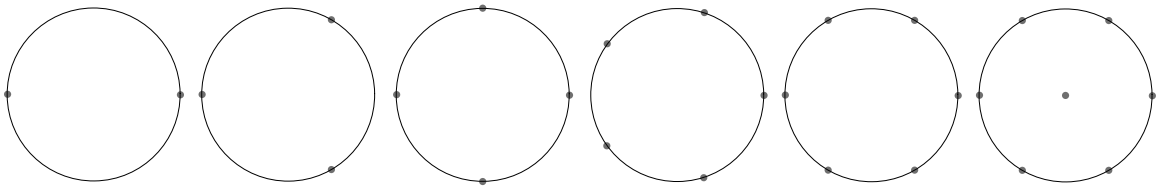

Figure 15: Optimal point arrangements in a circular container for $n = 2, \ldots, 7$ [Spe25].

Lemma 2.3. *Let $p_1, \ldots, p_n$ be n points lying in the unit disk. Then some pair of points is at distance at most*

$$\max\left(1,\ 2\sin\left(\frac{\pi}{n}\right)\right).$$

Proof. First, if some point p lies in the convex hull of a pair of points $\{p_j, p_k\}$ (Figure 16, on the left), then its distance to one of them is at most 1, and the lemma follows.

If p lies in the convex hull of more than two points, then it belongs to the triangle formed by some three of these points. In that case, p is at distance at most 1 from one of them (see Figure 16, middle).

Otherwise, every point p of the arrangement is outside the convex hull of the remaining points. Therefore, p can be moved radially outward until it lies on the boundary of the unit disk, without decreasing any of its distances to the other points, as shown on the right of Figure 16. Thus, we may assume that all points $p_1, \ldots, p_n$ lie on the boundary of the unit disk.

The points divide the circumference into n arcs. The total circumference is 2π, therefore, at least one arc has length at most $\frac{2\pi}{n}$. The chord subtended by such an arc has length at most $2\sin\left(\frac{\pi}{n}\right)$, which yields the desired upper bound. □

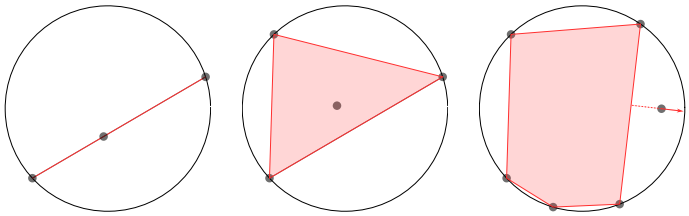

Figure 16: Illustration of the proof of Lemma 2.3.

For $1 < n \leq 6$ points, one has $\sin\left(\frac{\pi}{n}\right) \geq \frac{1}{2}$, and therefore, Lemma 2.3 implies that $d_n \leq 2\sin\left(\frac{\pi}{n}\right)$. The arrangements where all points lie on the boundary are thus optimal with $d_n = 2\sin\left(\frac{\pi}{n}\right)$.

For $n = 7$, the optimal configuration consists of six points on the boundary and one point at the center, $d_7 = d_6 = 1$.

The analogous proofs for higher number of points are significantly more complicated. As of today, such proofs were given for n from 2 to 10 [Pir69], 11 [Mel94], 12 [Fod00], 13 [Fod03], and 19 [Fod99]. Figure 17 represents these optimal packings. Pink disks, called *rattlers*, are free to move, yielding a continuum of optimal packings.

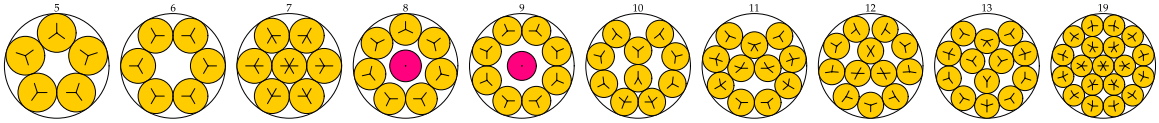

Figure 17: Optimal disk packing in a circle for $n = 5, \ldots 13$, and 19 [Spe25].

2.8. **Proving optimality by computer**

For the square container, starting from $n = 10$ (with a few exceptions), the optimality proofs rely on computer assistance. In this section, we use the case $n = 10$, proved in [PWMdG92], as an example. We will first sketch how to obtain a certified enclosure of the optimal point arrangements using the so-called *cell elimination method*, and then describe how the uniqueness of the optimal value inside this enclosure is proved via *shrinking error regions*.

We begin with a good lower bound $\underline{d}$ on d_n (for instance, for $n = 10$, one may take $\underline{d} = 0.42$). This bound is provided by a feasible candidate packing obtained in the previous step (Section 2.6). Using this value, we decompose the unit square into tiles of diameter at most $\underline{d}$, which guarantees that each tile can contain at most one point. In our example we use 16 tiles of size $\frac{1}{4} \times \frac{1}{4}$.

We then choose a combination of n *active* tiles, i.e., tiles that are candidates for containing a point, among the tiles of the decomposition (for $n = 10$ with 16 tiles this

yields $\binom{16}{10}$ possible choices). Figure 18 (left) shows one example of such a combination of active tiles (in white).

Each tile is then partitioned into a grid of small cells (for instance, an 8×8 square grid). A cell is declared active if it may contain a point under the current combination. The elimination step proceeds as follows: if a point were located in a given cell (i_0, j_0) (red in Figure 18) of some tile t_0 then every cell (i, j) in a neighbor tile which violates

$$(\,|i - i_0| + 1\,)^2 + (\,|j - j_0| + 1\,)^2 \;\geq\; (8\,\underline{d})^2$$

cannot contain a point. Indeed, the above inequality means that every point of (i_0, j_0) is at distance at most $\underline{d}$ from every point in (i, j).

Thus, each cell of t_0 induces an exclusion region in adjacent tiles. By intersecting all such exclusion regions we get the set of cells incompatible with the presence of a point in t, which can thus be eliminated altogether (you can see this eliminated set in Figure 18, for the bottom left active tile). If, after performing these eliminations tile by tile, active cells still remain in each tile, the grid is refined by subdividing each active cell into four smaller ones, and the elimination procedure is repeated.

If this iterative process eliminates all active cells in some tile for a given tile combination, this combination cannot correspond to an optimal packing. Otherwise, we obtain a validated enclosure of the true optimum, as in Figure 18, on the right.

For $n = 31$–33, certified enclosures are the best results available so far [Mar21]. For smaller values of n, however, the precise structure of the optimal arrangement (or the set of optimal arrangements, as in cases with rattlers) is known for all n up to 30 and for $n = 36$.

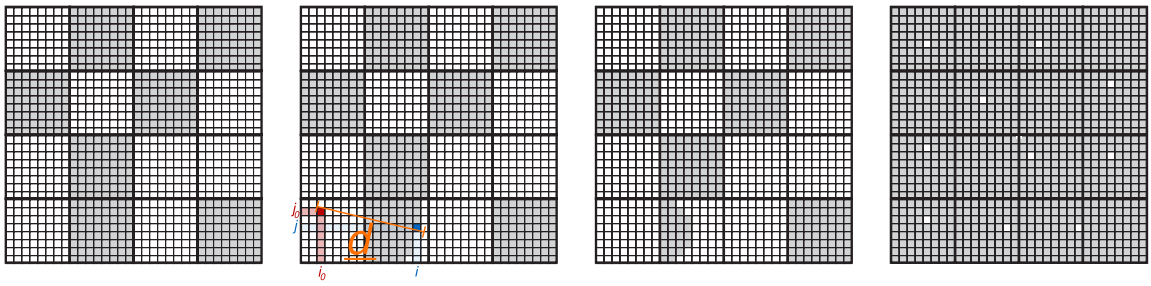

Figure 18: Illustration of active cell elimination process for $n = 10$.

We switch from points arrangements to disk packings for this part. The proof of uniqueness follows a procedure structurally similar to the elimination method above, but instead of working with square cells we use convex regions bounded by straight lines and circular arcs. We begin by "guessing" the tangency graph of the optimal

packing. From these tangencies we obtain approximate center positions, and around each guessed center we place an initial error region: a disk of small error-radius ε (white in Figure 19, on the left). These regions represent the admissible locations of the centers in the optimal packing.

The elimination step now proceeds by cutting these error regions with straight lines. Given two neighboring circles C_i and C_j, the region R_i can be used to remove from R_j all points that cannot satisfy the tangency constraint with any point of R_i. The endpoints of each cutting line are determined by examining all critical points on the boundary of R_i. After performing all such cuts among all neighboring pairs, each region becomes a convex polygon strictly contained inside its original error disk (see Figure 19, in the middle).

At this stage, all regions have shrunk by a common contraction factor $q < 1$, so the radii of the error disks can be updated from ε to $q\varepsilon$. It turns out that, after scaling all regions by this factor, the same sequence of cuts can be applied again. Iterating this process produces a nested sequence of concentric shrinking error-disks, and these converge to the unique packing compatible with the guessed tangency pattern. In this way, the optimal packing is shown to be unique.

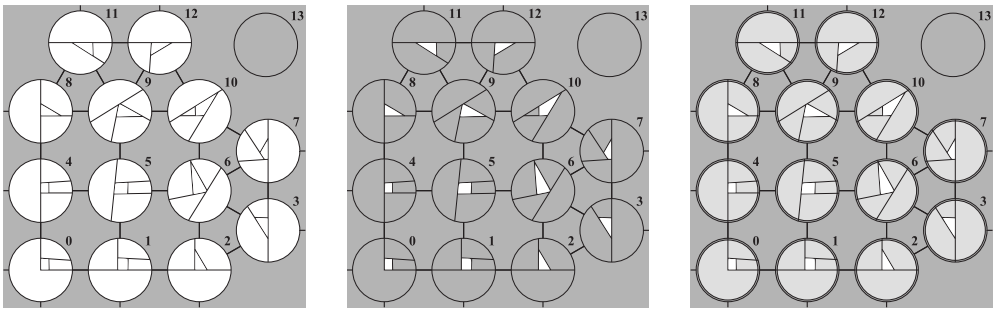

Figure 19: Example of shrinking error regions during the uniqueness proof for $n = 13$ from [PWMdG92].

2.8.1 **Optimal disk packings in squares**

Figure 20 illustrates packings of n unit disks in a square proved to be optimal for $n = 4, \ldots, 30$ and 36. For $n =$ 1–9, the proof was obtained by hand [SM65, Sch70], as well as for $n = 14, 16, 25, 36$ [KW87, Wen83, Wen87b, Wen87a]. Computer-assisted methods seen above were used for $n =$ 10–20 [dGPW90, PWMdG92], for $n =$ 21–27 [NO99], and for $n =$ 28–30 [Mar07]. Notice that for $n = 28$ and 29, even though the exact combinatorial structures (tangencies) of the globally optimal packings are known, the exact solution of the algebraic systems of equations needed to

obtain symbolic expressions for the coordinates (and the optimal value of the objective function) has not yet been found. Consequently, these packings are described by their structure together with very tight enclosures of the centers.

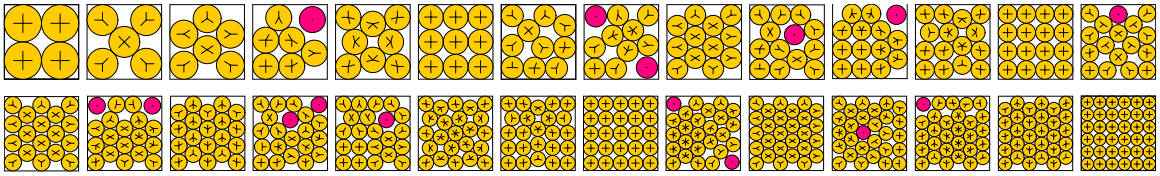

Figure 20: Optimal packings of n disks in a square for $n = 4$–30 and 36 [Spe25].

Figure 21 depicts the cases $n = 31$–33 with certified enclosures for the optima. The width of each enclosure is at most 10^{-11}, so the disk centers are shown as points: the enclosure is invisible to the eye, although some of the indicated tangencies may not occur in the true optimum (the structure of the packing is not fully determined). These results are due to [Mar21].

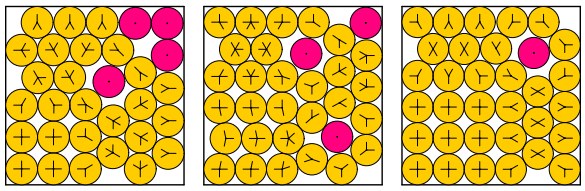

Figure 21: Certified enclosures of optimal packings for $n = 31$–33 [Spe25].

3. **Triangulations and scissors**

Let us turn to infinite packings. This setting is different from container problems, in particular, the mathematical program would involve infinitely many variables and there is no bounded domain. Nevertheless, we will see that some methods are common for both.

Let S be a set of disks. A *plane packing* of disks from S is a configuration of copies of disks from S on the plane such that the disks do not overlap. To measure the proportion of the plane covered by an arrangement, we introduce the notion of *density*. Let P be a packing and let X be a compact subset of the plane. The *density of P inside X*, denoted $\delta|_X(P)$, is formally defined as

$$\delta|_X(P) := \frac{\text{area}(X \cap P)}{\text{area}(X)}.$$

The *density of the packing* P, denoted $\delta(P)$, is the proportion of the plane covered by the disks of the arrangement.

$$\delta(P) := \limsup_{n\to\infty} \delta|_{B_n}(P),$$

where B_n denotes the disk of radius n centered at the origin.

Our main problem is the following: given a set of disks S, find the maximal density of an arrangement of the plane with these disks. We denote this value by δ_S and formally define it as follows:

$$\delta_S := \sup_{P \text{ is a packing by } S} \delta(P).$$

Any packing that reaches the maximal density is called *optimal*.

3.1. **One-disk packings**

Let us return to the subject with which we began: packings of identical disks (or *one-disk packings*). For simplicity, we consider arrangements of unit disks.[6] As mentioned in the Section 1, the hexagonal packing, represented in Figure 22a, is optimal. This was formally proved in 1942 by Fejes Tóth [FT42]. The density of the hexagonal packing is equal to

$$\delta_{\text{hex}} := \frac{\pi}{2\sqrt{3}} \approx 0.9069 \approx 91\%.$$

We will now see how to prove this result. Our goal is to demonstrate that no packing of unit disks is denser than the hexagonal one. A disk arrangement on the plane is an infinite object, so we have to analyze an infinite number of infinite objects... To make our problem a bit less "infinite", we cut each packing into small pieces and show that none of these pieces is denser than $\delta_{\text{hex}} = \frac{\pi}{2\sqrt{3}}$.

This will conclude the proof: indeed, once the density of each individual piece is bounded, the density of every finite portion of the packing is bounded by the same value, and by definition this bounds the density of the entire packing. Therefore, no packing of unit disks in the plane can be denser than the hexagonal packing.

A packing P of disks from S is called *saturated* if it is impossible to place more copies of disks from S on the plane without intersecting the disks in P. From now on, we only consider saturated packings: indeed, inserting disks in a packing does not decrease the density, so an upper bound on the density of saturated arrangements is an upper bound for all arrangements. Figure 22 represents saturated packings; examples of non-saturated 2-disk arrangements are given in Figures 26a and 26c.

[6]The density of an arrangement does not change if a homothety is applied.

There are two natural ways to cut a packing into pieces, leading to two distinct proofs: one based on polygons and another based on triangles.

The first approach is to use the Voronoi diagram to partition the packing, as we already did for packings in containers in Section 2. To obtain an upper bound on the maximal pairwise distance, we rely on the fact that the smallest Voronoi cell of a unit disk is the circumscribed regular hexagon, whose area equals $2\sqrt{3}$ [Rog58]. Hence, the density inside any Voronoi cell of a unit disk in a packing is at most $\frac{\pi}{2\sqrt{3}}$, which completes the proof.

The second method, used in [Thu10] and [FT53], is to decompose the arrangement into triangles whose vertices are the centers of the disks. Let us draw the *dual graph* of the Voronoi diagram: its vertices correspond to the disk centers, and two centers are connected by an edge if and only if their Voronoi cells share a boundary. This graph, shown in black in Figure 22, is called the *Delaunay triangulation* [Del34] of the packing.[7]

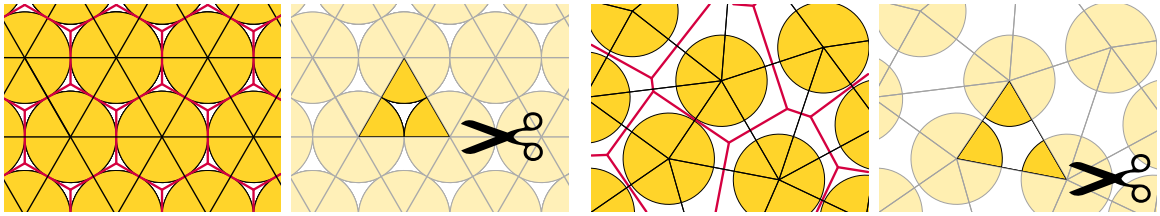

(a) Hexagonal arrangement. (b) Another saturated arrangement.

Figure 22: Voronoi Diagrams and Delaunay triangulations.

It turns out that, by fundamental properties of Delaunay triangulations of saturated arrangements, the area of any Delaunay triangle is at least $\sqrt{3}$.[8] The intersection of such a triangle with the disks of the packing consists of three circular sectors whose angles sum to π. Hence, the total intersection area is always $\frac{\pi}{2}$. Then the density of each Delaunay triangle is at most $\frac{\pi/2}{\sqrt{3}}$, which completes our second proof.

3.2. **2-disk packings**

Now that we know the optimal packing of identical disks, in addition to the unit disks (), let us also use copies of a second, smaller, disk of radius r (). The maximal density of *two-disk* packings with the unit disk and the small r-disk is denoted δ_r.

[7] More precisely, one can always obtain a triangulation from the dual graph. For an algorithmic perspective on Delaunay triangulations, see [GO04].

[8] A simple proof of this fact can be found in [CW10].

For certain values of r, the optimal packings are known: for instance, the 9 arrangements depicted in Figure 27. For other values, the maximal density δ_r is still unknown, so we at least try to find bounds for it. For example, by using only one of the disks, we can always achieve the density of the hexagonal arrangement $\delta_{\text{hex}} = \frac{\pi}{2\sqrt{3}}$; this gives us a lower bound for the maximal density regardless of the radius of the small disk. This bound is traced in green in Figure 25.

The use of the second disk potentially allows for a density greater than δ_{hex}. For example, if the small disk fits into the gap between three pairwise tangent large disks, placing a small disk in each gap of the hexagonal arrangement strictly increases the density[9]. On the other hand, if the radius of the small disk approaches 1, the use of the second disk does not increase the maximal density.

The definition of the Delaunay triangulation extends quite naturally to arrangements with multiple disk sizes. This generalization, introduced in [FTM58], is called the *FM-triangulation*. The only novelty in this setting is that a Voronoi cell is defined as the set of points closer to a given disk than to any other disk in the packing; thus, an edge separating two disks of different radii is a hyperbolic arc rather than a straight line[10].

Florian used this triangulation to obtain an upper bound on the maximal density of a two-disk packing [Flo60]. He showed that, regardless of the arrangement, no triangle of its triangulation is denser than the triangle formed by two small disks and one large disk, all mutually tangent. Figure 25 (in blue) traces the Florian bound on the maximal density as a function of the value of r.

Nine years later, Blind obtained another bound using a different cutting rule: he considered *power diagrams* rather than Voronoi partitions or FM-triangulations [Bli69]. The *power* Π of a point X with respect to a disk D is the square of the distance from X to D, more formally, it is defined as

$$\Pi_D(X) := |OX|^2 - R^2,$$

where O is the center and R the radius of the disc. Given a packing P, its *power diagram* is a partition of the plane into *power cells* associated to the discs; each cell consists of the points whose power distance to a given disk is smaller than to any other disk in P. The cells of the power diagram are all convex and polygonal.

Note that the power diagram of a packing of identical disks coincides with its Voronoi partition. Figures 23, 24 depict respectively the Voronoi partition and the

[9]Moreover, if the size of the small disk tends to zero, we can pack the small disks in a hexagonal manner inside the gaps and obtain the density $\delta_{\text{hex}} + (1 - \delta_{\text{hex}})\delta_{\text{hex}} \approx 99\%$.

[10]For more details, the reader may consult Chapter VI of Fejes Tóth's book [FT64]. Readers who read German may also refer to the original paper [FTM58].

power diagram of a disc packing.

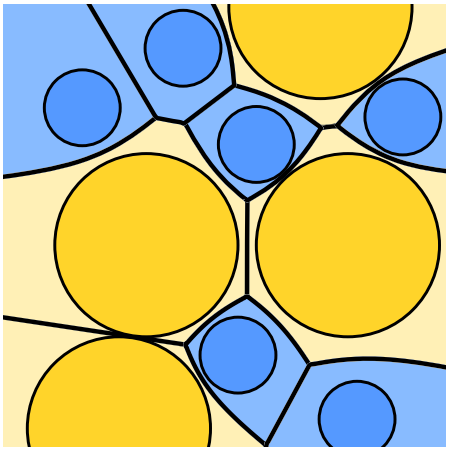

Figure 23: The Voronoi partition.

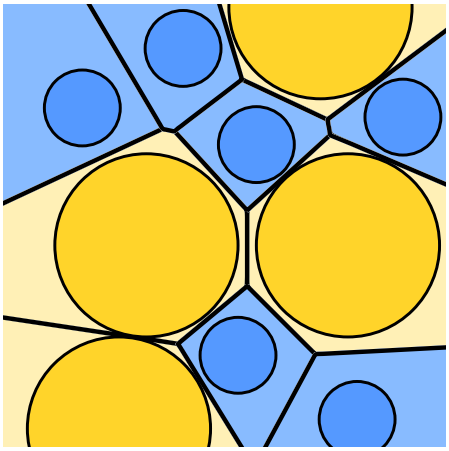

Figure 24: The power diagram.

Blind bounded the maximal density of an arrangement by the density of the union of a regular heptagon circumscribed around a unit disk and a regular pentagon circumscribed around a disk of radius r. The Blind bound is traced in red in Figure 25; note that this bound provides a threshold $q_B \approx 0.74$ (•) such that for any r greater than q_B, the densest arrangement is the hexagonal arrangement using only a single disk size.

3.3. **Triangulated packings**

Finding optimal packings for each pairs of disk sizes is difficult. Let us start from the other end: which packings seem very dense? We have shown that for identical disks, the hexagonal packing is optimal. Its triangulation is composed of identical triangles formed by three mutually tangent disks (Figure 22a). Let us generalize this property.

First, we define the *contact graph* of a packing as a graph whose vertices are the centers of the disks and each edge corresponds to a pair of tangent disks (Figures 26c–26d depict four examples of arrangements with their contact graphs). A packing is called *triangulated* if its contact graph is a triangulation, i.e., all its faces are triangular; Figures 26c, 26d show two examples of triangulated arrangements. An informal definition is that each of the "gaps" of a triangulated packing is delimited by three mutually tangent disks. As illustrated by Figure 26, the properties of being triangulated or saturated are orthogonal.

In [FT84], Fejes Tóth calls triangulated arrangements "compact": they do not have large gaps, so they intuitively seem to be the most compact. Furthermore,

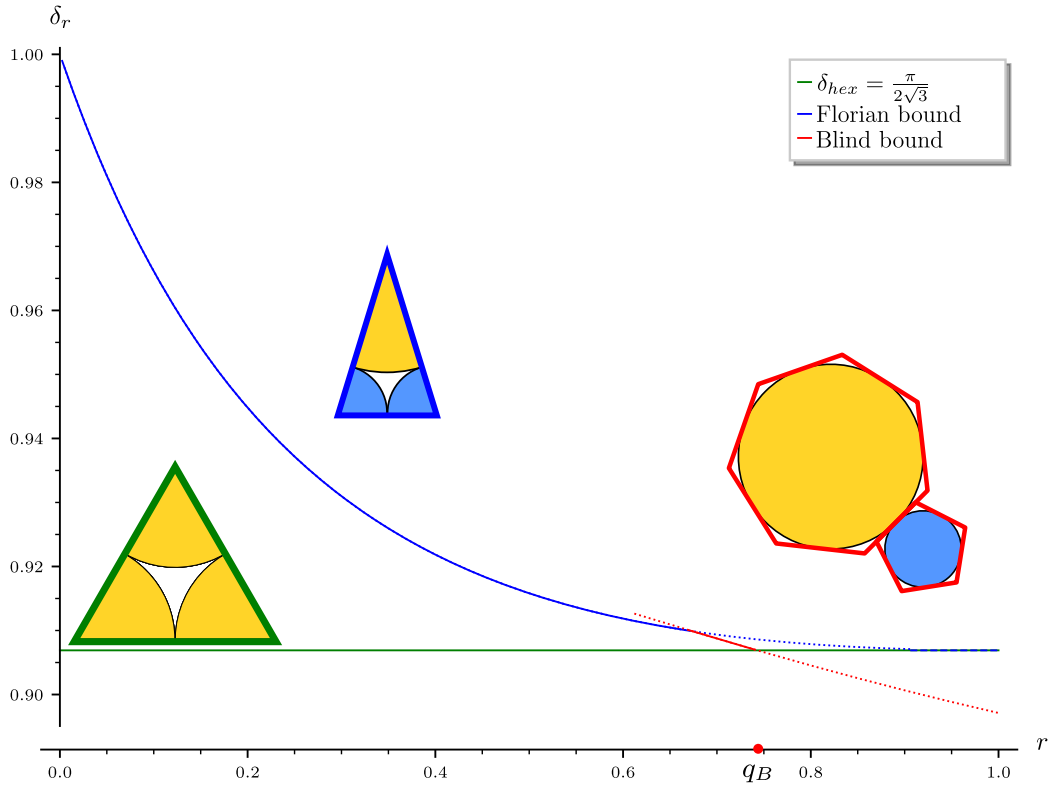

Figure 25: The bounds of Florian (in blue) and Blind (in red) as well as the density of the hexagonal arrangement (in green). The radius q_B (•) is the threshold value of r above which the hexagonal arrangement is optimal: i.e., the use of the second disk does not increase the maximal density.

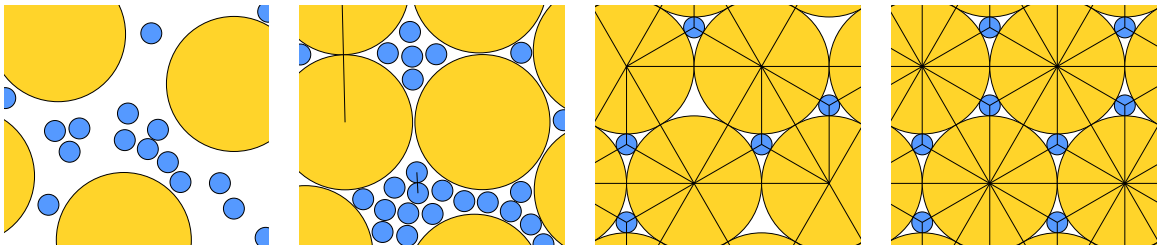

(a) Non-saturated non-triangulated.

(b) Saturated non-triangulated.

(c) Non-saturated triangulated.

(d) Saturated triangulated.

Figure 26: Examples of packings.

around each disk, its neighbors form a "crown" of tangent disks that appear to be a locally optimal configuration. For these reasons, saturated triangulated packings seem to be the best candidates for maximizing density.

We call a value of r *triangulated* if it allows for triangulated packings using both

unit disks and disks of radius r. Not all values of r are triangulated: to understand this, we invite the reader to try to arrange coins of two sizes on a table in a perfectly triangulated manner[11].

In 2006, Kennedy demonstrated that there are only 9 values of r allowing triangulated packings in which both disk sizes are present. We denote these values by $r_1, \ldots, r_9$; their corresponding triangulated packings are shown in Figure 27. Each of these packings is *periodic*, meaning that there exist two non-collinear vectors, called periods, such that translating the packing by either vector leaves it unchanged. In this work, we always consider packings of the entire plane, and since the triangulated packings depicted here and below are all periodic, it is sufficient to represent their fundamental domain (a parallelogram spanned by the period vectors, marked in black in Figure 27) to see how the entire plane is packed.

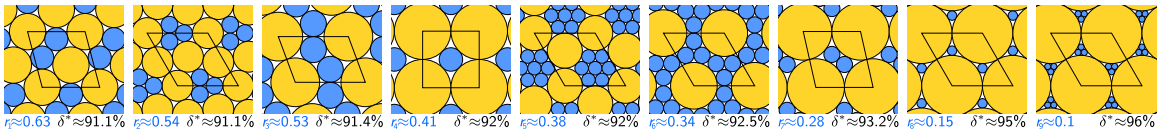

Figure 27: Periodic triangulated binary packings corresponding to cases $b_1, \ldots, b_9$.

A pair of disks with radii $1, r_i$, $i \in \{1, \ldots, 9\}$ is called a *binary case*. The binary cases are designated by $b_1, \ldots, b_9$. It turns out that for each of the nine binary cases, the density is maximized by a triangulated binary disk packing — one of those shown in Figure 27[12]. Heppes in [Hep00] showed that the triangulated disk packing of b_4 (represented in Figure 27), where $r_4 = \sqrt{2} - 1$, maximizes the density among all two-disk packings with disks of radii 1 and r_4. Three years later, Heppes generalized his method to cover five other cases: b_1, b_3, b_6, b_7 and b_8 [Hep03]. Despite his efforts, that proof is difficult to understand due to the complex case analysis carried out by hand; this is why subsequent results in the area are computer-assisted. Indeed, separating the proof into a sequence of clear, human-readable ideas from the computer code handling the case enumeration allows both better understanding and greater reliability. The next step was made by Kennedy, who introduced the method of *localizing potentials*, inspired by the potentials of classical statistical mechanics. This new approach allowed him to treat b_2 [Ken05]. Finally, the fully computer-assisted method required to solve the two remaining triangulated cases, b_5 and b_9, was provided by Bedaride and Fernique [BF22].

[11] In reality, using two-euro and one-cent coins, one can approximate a triangulated arrangement... The motivated reader is invited to find it.

[12] These packings are not the only triangulated packings corresponding to the triangulated radii r_i. There is an infinite number of triangulated packings for certain radii, as described in [Ken06].

By modifying the method used in the previous result, Fernique obtained new bounds on the density, which provide an almost complete description of the behavior of the maximal density as a function of the size of the small disk r [Fer22]. These bounds are shown in Figure 28.

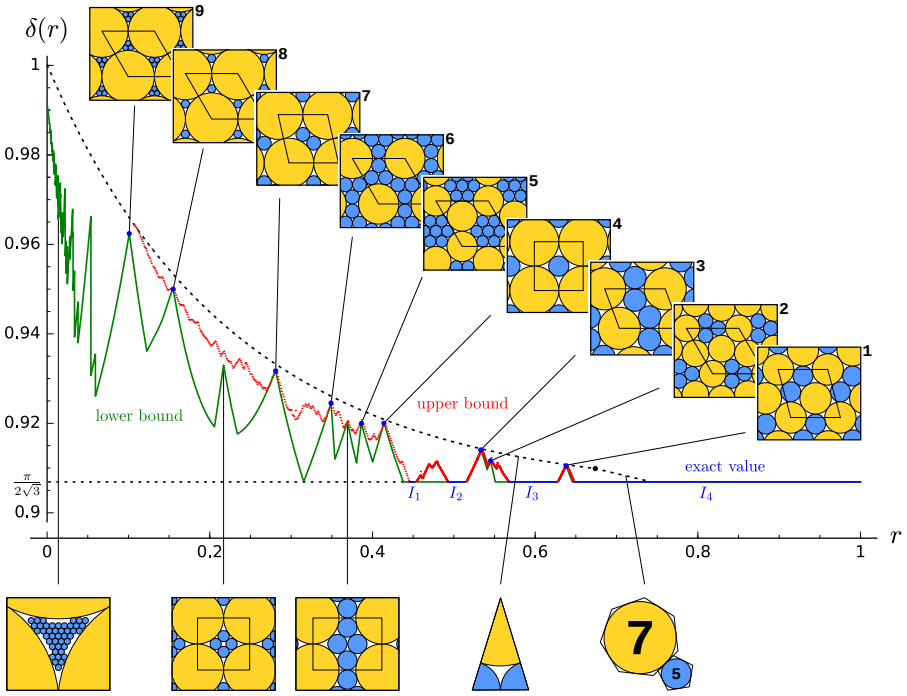

Figure 28: The Fernique bounds.

3.4. **3-disk packings**

Using more disk sizes potentially allows for denser packings, but it also increases the combinatorial complexity of the problem which complicates the study. We saw earlier that the hexagonal packing, the only triangulated packing of identical disks, is optimal. We also learned that whenever a pair of disk sizes admits a triangulated packing, a triangulated packing is in fact optimal. These results naturally suggest the following conjecture.

Conjecture 3.1 (Connelly, 2018 [CGSY18])**.** *If a finite set of disks allows a saturated triangulated packing, then the density of a packing using these disks is maximized by a triangulated packing.*

As the statement above is true for one-disk packings and two-disk packings, the next step is to verify it for three-disk packings (or *ternary packings*). First, we must

find the disk sizes allowing triangulated ternary packings. This problem was solved in 2021: there are 164 pairs (r, s) allowing triangulated packings with disks of radii $1, r, s$, $1 > r > s$ [FHS21].

Here and later, a triplet of disks with the radii associated with each of these pairs is called a *triangulated triplet*. Triangulated triplets are indexed by positive integers from 1 to 164, as in [FHS21].

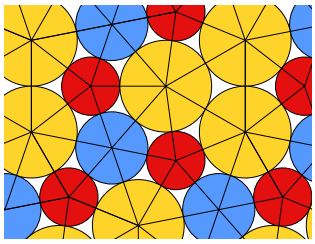

Figure 29: The triangulation of a triangulated packing and two of its triangles.

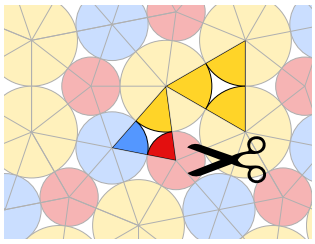

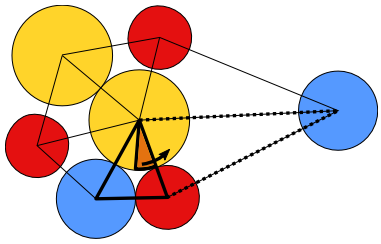

Figure 30: Illustration of density redistribution.

Unlike one-disk packings, a simple triangulated partition is not sufficient to demonstrate the optimality of a multi-disk packing. This is due to the fact that a packing with multiple disk sizes feature several types of triangles (Figure 29), some of which are denser than the density of the triangulated packing. To obtain the proof of optimality, we use a method which was called "cell balancing" in [Hep03]; it consists in redistributing the density among the triangles. Indeed, even if certain triangles are particularly dense, some of their neighbors are very "empty," as illustrated in Figure 30. The method has two steps: first, we locally redistribute the density among selected cells while preserving the global density. Then we prove that, after redistribution, the density of every triangle in the packing remains below the target density.

Computer assistance is required for several parts of the proof: an extensive case analysis and symbolic computations are needed to construct the redistributed density function, and interval analysis combined with recursive subdivision (as introduced in the context of packings in containers in Section 2.8) is then used to verify the density bound over the entire space of possible triangles.

This method yields a proof of optimality for the 16 packings shown in Figure 31 [FP23]. It also established the optimality of the two-disk triangulated packings depicted in Figure 27 for 16 triplets from Figure 32. These are the cases were introducing the third disk size (blue disk) does not increase the maximal density.

The bad news is that the conjecture is false: there are at least 45 counterexamples. When the ratio between two of the three disks is close to that of an optimal binary packing, it is possible to arrange the three disks in a similar (non-triangulated) way

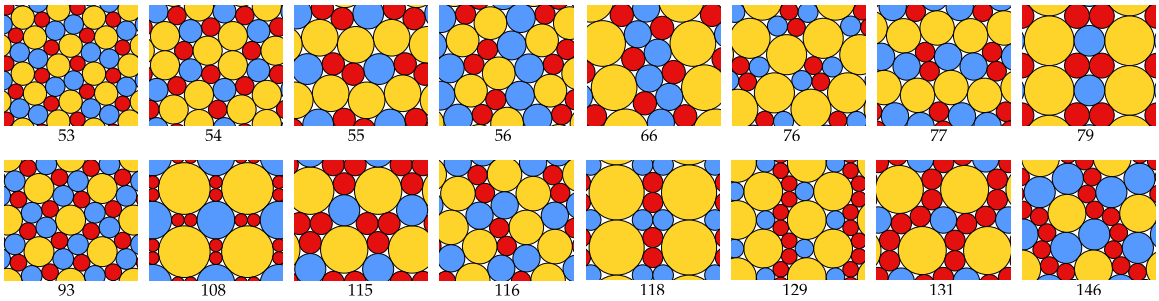

Figure 31: Optimal three-disk packings.

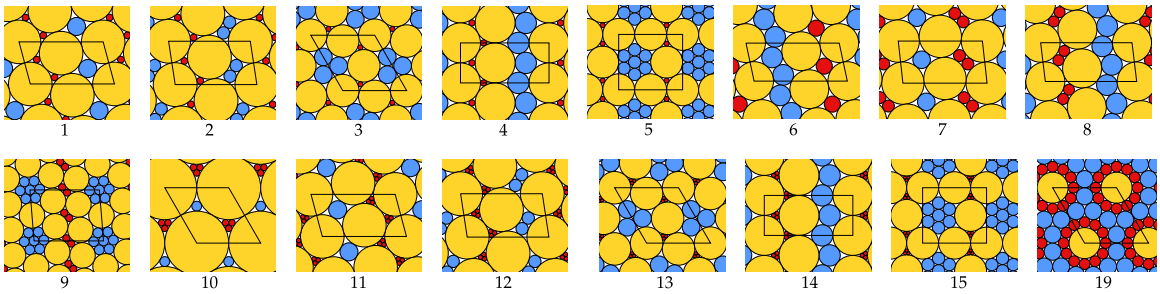

Figure 32: The ternary cases where the optimal packings use only two out of three disks. For cases 1 to 5, this is the triangulated packing of b_8 (Figure 27); for case 6 — b_4; for cases 7 to 9 — b_7; for cases 10 to 15 — b_9; for case 19 — b_6.

and still obtain a high density. The density of triangulated binary packings (represented by Figure 27) exceeds the density of the majority of triangulated ternary packings, which suggests using them to find counterexamples (that is, disk triplets having a non-triangulated packing that is denser than any triangulated packing).

The pairs of disks allowing binary triangulated packings are designated by $b_1, \ldots, b_9$, while the triplets with ternary triangulated packings are indexed by positive integers from 1 to 164. Let us illustrate this method with an example. Take case 73; its triangulated ternary packing is shown in Figure 33, on the right. Notice that the radius of the smallest disk ($s_{73} \approx 0.264$) in case 73 is close to the radius of the small disk ($r_{b_7} \approx 0.281$) in case b_7.

We deform the binary triangulated packing b_7 (Figure 33, on the left), by replacing the small disk of b_7 with the smallest disk of case 73. These deformations are inspired by the flip-and-flow method introduced in [CG21][13]. We choose a deformation that breaks the fewest contacts between the disks, it is given in the center of Figure 33. Notice that the only broken contact is between the pair of red disks: they are no longer

[13]Flip is for flipping an edge in the contact graph of the packing, flow — for the continuous deformation which follows.

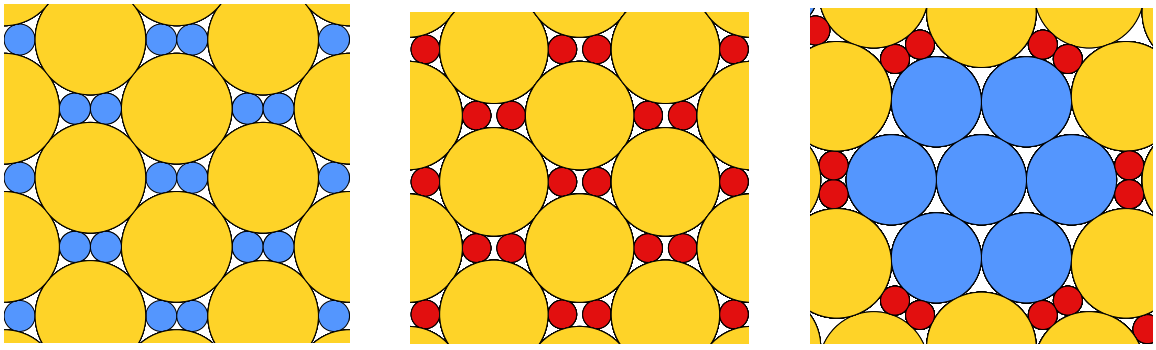

Figure 33: On the left: a binary triangulated packing of case b_7. In the middle: its deformation where the small disks are replaced by the smallest disks of case 73. On the right: a periodic triangulated packing of case 73, its fundamental domain and its description are given in [FHS21].

tangent. The density of the deformed packing is slightly higher than the density of the triangulated ternary packing, making it a counterexample.

4. Salt, tetrahedra and computer

4.1. One-sphere packings

The packing of "cannonballs" described by Kepler in his manuscript [Kep11] is known today as the *face-centered cubic packing* (or FCC). It is a regular packing: the centers of the spheres are arranged at the vertices of the FCC lattice, which gave the packing its name. Figure 34, on the left, depicts the local configuration of the FCC packing. An equally dense compact packing generated by another regular lattice, the *hexagonal close-packing* (or HCP), was first mentioned by Barlow in 1883 [Bar83] (Figure 34, on the right). There is actually an infinite family of globally distinct compact packings, all having the same density

$$\frac{\pi}{3\sqrt{2}} \approx 0.7404 \approx 74\%,$$

they are called the *close-packings*. Every close-packing is constructed by stacking layers of spheres whose centers form the hexagonal lattice on the plane; each new layer can be placed in two different ways relative to the two previous layers (see Figure 35), so we obtain an uncountable number of packings in the end. There are, however, only two local configurations around a sphere, represented by Figure 34, that appear in close-packings; their Voronoi cells are both of density $\frac{\pi}{3\sqrt{2}}$.

Gauss in 1831 [Gau31] established a link between lattices and quadratic forms

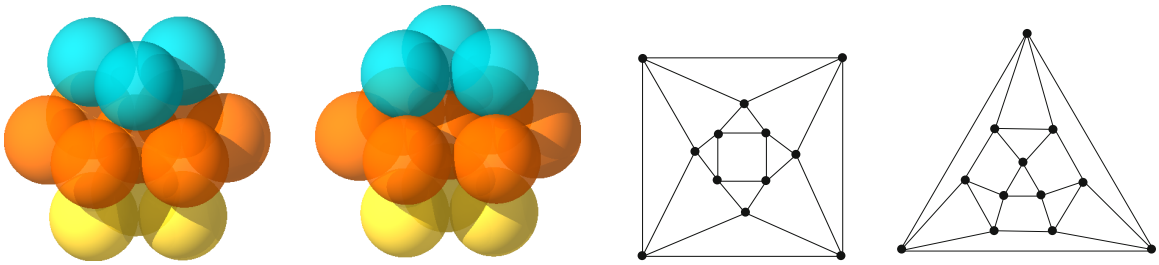

Figure 34: FCC (left) and HCP (right) local configurations of spheres and their contact graphs.

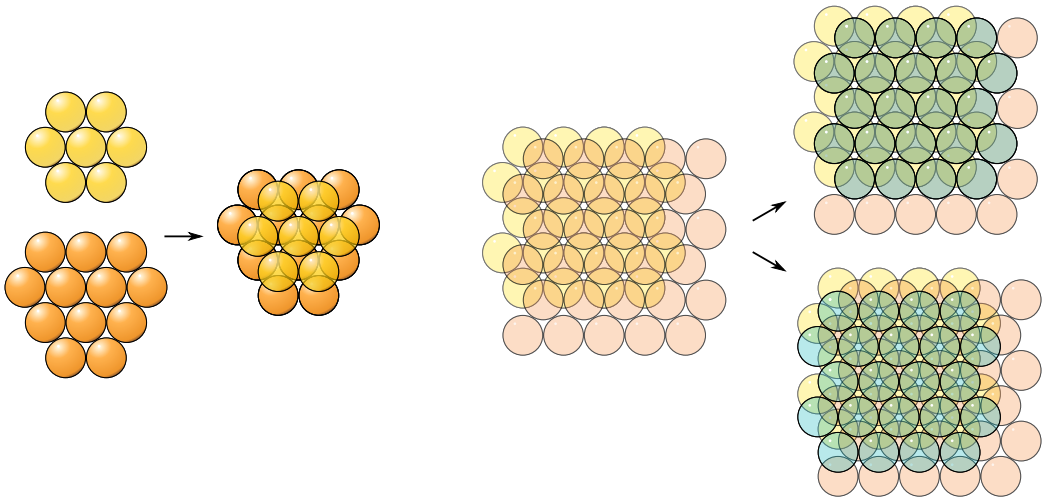

Figure 35: Layer-by-layer construction of compact packings of congruent spheres.

which implied that compact packings maximize the density among lattice packings[14]. The general result turned out to be much more difficult. The conjecture remained open for 400 years, and was even included in Hilbert's list of problems as part of the 18^{th} problem [Hil02]. In the following years, researchers used various approaches to obtain increasingly tighter upper bounds on the maximal density of sphere packings. Blichfeldt obtained the first upper bounds (0.884 and 0.835) in 1919 and 1929 [Bli19, Bli29]. In 1958, Rogers bounded the density of a packing by the density inside the tetrahedron formed by four pairwise tangent spheres (we call such tetrahedra *tight tetrahedra*), equal to ≈ 0.7796, [Rog58]. The best upper bound before the resolution of the Kepler conjecture was given by Muder [Mud93] and is ≈ 0.773055.

The Kepler conjecture is a continuous optimization problem (we are trying to maximize the density function over the set of all packings) with an infinite number of variables (there are an infinite number of spheres to pack). László Fejes Tóth

[14] i.e. those where sphere centers form a lattice

took a great step towards the proof of the Kepler conjecture by proposing to use the local density approach [FT53]. This approach makes it possible to reduce this infinite-dimensional optimization problem to one having a finite number of variables. Furthermore, he was the first to suggest the use of a computer; in his book on regular figures [FT64], he writes:

> Given the complexity of this function, we are far from attempting to determine the exact minimum. But, aware of the rapid development of our computers, it is imaginable that the minimum could be approximated with great accuracy.

The initial approach by Hales to the Kepler conjecture [Hal92, Hal93] was based on the Delaunay partition of space but did not lead to a complete proof. He therefore adopted a hybrid partition involving Delaunay simplices together with modified Voronoi cells. In collaboration with Ferguson, Hales completed the first full version of the proof in 1998. The global idea of the proof is similar in spirit to the density redistribution method we saw for disk packings, but in three dimensions everything becomes far more complicated; extensive computer assistance is required for several parts of the argument. The proof consisted of six preprints and tens of thousands of lines of computer code. It took several years of intensive reviewing before the team of 12 referees declared themselves "99% sure" of its correctness, and a fully revised complete version was finally published in 2006 [HF06]. In the meantime, an abridged version of the proof had appeared in the Annals of Mathematics [Hal05].

In 2003, Hales launched a global collaborative project to obtain a formal proof of the Kepler conjecture. The project was named Flyspeck, which is an expansion of "FPK", for "the Formal Proof of the Kepler conjecture". The goal of the project was to construct a complete formal proof verifiable by proof assistants such as HOL Light and Isabelle. Flyspeck was completed in 2014; three years later, after meticulous review by the mathematical community, the formal proof was accepted by the Forum of Mathematics [HAB+17].

You will find detailed insights on the history of the Kepler conjecture and its proof up to 2003 in Szpiro's popular book [Szp03].

4.2. **Two-sphere packings**

In 2D, the only non-trivial tight bounds on the maximal density of disk packings have been obtained for cases where triangulated packings maximize the density. Indeed, having a relatively simple combinatorial structure of the contact graph in the optimal packings simplifies the problem. The three-dimensional version of triangu-

lated packings are the *simplicial packings* — those whose contact graphs decompose into tetrahedra.

The study of simplicial packings in higher dimensions is carried out in [KM23], which generalizes the two-dimensional result of [Mes23] to arbitrary dimension. The authors show that for any dimension d and any number n, the set of n-tuples $r_1, \dots, r_n$ with $r_1 < \dots < r_n = 1$ for which there exists a simplicial packing in $\mathbb{R}^d$ by spheres of radii $r_1, \dots, r_n$ (with spheres of each of the n sizes actually present) is finite. As we have seen, there are only 9 radii r with triangulated two-disk packings and 164 pairs (r, s) with triangulated three-disk packings.

Close-packings in 3D are not simplicial: the contact graphs of the two local configurations around a sphere, represented in Figure 34, have quadrilateral faces. Therefore, non-triangular faces are present in the contact graph of any close-packing. Unlike disk packings, there is no simplicial packing of identical spheres in 3D.

It turns out that the only value $r < 1$ allowing simplicial packings by unit spheres and r-spheres is $\sqrt{2} - 1$ [Fer21]. The simplicial packings of spheres of radii 1 and $\sqrt{2} - 1$, which we call *salt packings*, are constructed by taking a close-packing of unit spheres and filling its octahedral gaps with small spheres (an example is given in Figure 36), these are the orange and cherry packings from Section 1 (Fig 6). We call the pair of spheres of radii 1 and $\sqrt{2} - 1$, the *salt spheres*.

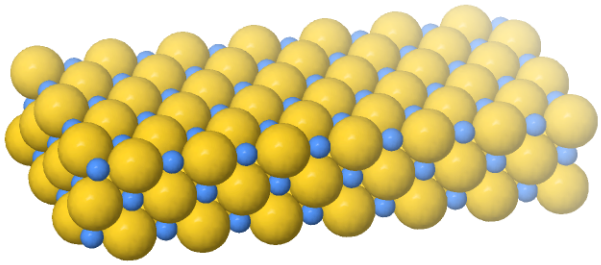

Figure 36: An example of a salt packing.

The name chosen for this class of packings comes from chemistry: *rock salt* is the name of mineral form of sodium chloride whose crystallographic structure corresponds to a face-centered cubic packing of chloride ions whose octahedral voids are filled with sodium ions. This structure is common among two-element crystals [Sei40].

All salt packings have the same density equal to

$$\delta_h := \frac{\pi}{3\sqrt{2}} \left(5\sqrt{2} - 6\right) \left(\frac{5}{3} - \sqrt{2}\right) \pi \approx 0.7931 \approx 79\%.$$

We conjecture that this density is optimal:

Conjecture 4.1. *Salt packings maximize the density among packings by spheres of radii* 1 *and* $\sqrt{2}-1$.

This conjecture seems like a very complex project, especially in light of the effort required to prove the Kepler conjecture. In cases where finding and proving an optimal packing appears out of reach, we at least aim to obtain bounds on the optimal value. Let us therefore derive a (non-tight) upper bound on the maximal density of packings by salt spheres.

Before turning to our geometric approach, let us mention the analytic method of Cohn and Elkies [CE03]. They use the Poisson summation formula together with a carefully chosen auxiliary function to obtain upper bounds on the packing density of the form $f(0)/\widehat{f}(0)$. For identical spheres this method gave record bounds in dimensions 4–24, coming within a factor of less than 1.001 of optimal in dimensions 8 and 24 [Via17, CKM+17], mentioned in the introduction. This result was extended to mixtures of sphere sizes in [DLDOFV14]. However, in low dimension, its precision is limited: in 2D it is weaker than geometric bounds such as Florian's (Section 3.2), while in 3D it yields an upper bound of 0.813 for packings of salt spheres, which is slightly worse than the geometric upper bound we explain below.

To obtain our upper bound, we follow the spirit of Florian's method. It consisted in bounding the packing density by the density inside the densest triangle; in 3D, we do the same with the density inside the densest tetrahedron. The 3D version of a triangulation, called a *simplicial partition*, is illustrated in Figures 37 and 38.

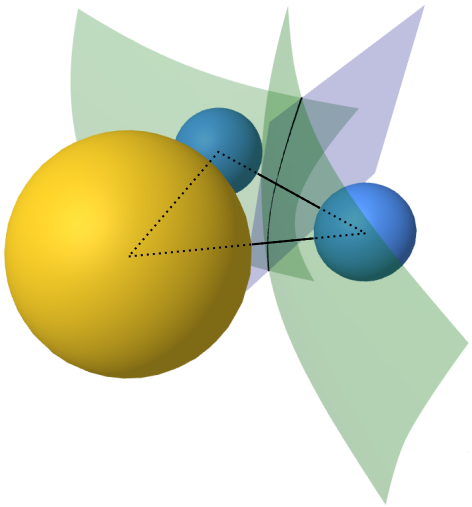

Figure 37: Boundaries of the Voronoi cells of a three-sphere configuration.

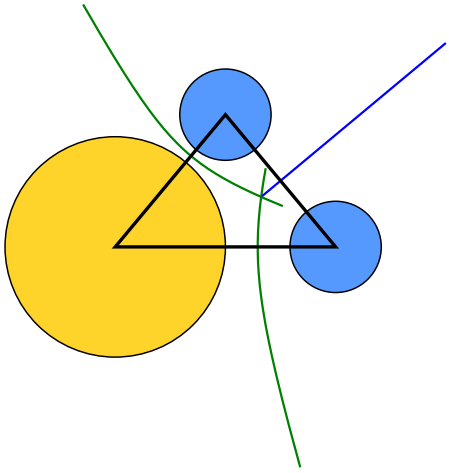

Figure 38: Intersection of this configuration with the plane passing through the centers of the spheres.

A detailed study of the geometric properties of tetrahedra in simplicial partitions of packings by salt spheres combined with challenging interval arithmetic computations (75 hours of CPU time on an average laptop), the densest tetrahedron for each quadruple of sphere radii was determined in [FP25].

Theorem 4.2. $r = \sqrt{2} - 1$ *Each of the following tetrahedra is of maximal density among those composed of the same spheres:*

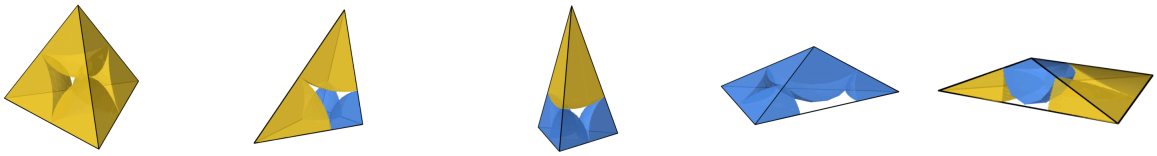

$\delta_{1111} \approx 0.72093$ $\delta_{11rr} \approx 0.81056$ $\delta_{1rrr} \approx 0.80650$ $\delta_{rrrr} \approx 0.78478$ $\delta_{111r} \approx 0.81254$

This theorem implies an upper bound on the maximal density of a packing by salt spheres, equal to the density of the densest of these tetrahedra:

$$\delta_{111r} \approx 0.81254202781083486694360052888335222033874855926335447.$$

This value is higher than the conjectured maximal density (0.793) because a salt packing, e.x., the one shown in Figure 36, consists of tight tetrahedra of types[15] 1111 and $111r$, rather than the densest tetrahedron of type $111r$, which does not tile space.

References

[Bar83] W. Barlow. Probable nature of the internal symmetry of crystals. *Nature*, 29:186–188, 1883.

[BDGL00] W. D. Boll, J. Donovan, R. L. Graham, and B. D. Lubachevsky. Improving dense packings of equal disks in a square. *The Electronic Journal of Combinatorics [electronic only]*, 7(1):Research paper R46, 9 p.–Research paper R46, 9 p., 2000.

[BF22] N. Bedaride and T. Fernique. Density of binary disc packings: The nine compact packings. *Discrete & Computational Geometry*, 67:1–24, 2022.

[Bli19] H. F. Blichfeldt. Report on the theory of the geometry of numbers. *Bulletin of the American Mathematical Society*, 25(10):449 – 453, 1919.

[Bli29] H. F. Blichfeldt. The minimum value of quadratic forms, and the closest packing of spheres. *Mathematische Annalen*, 101:605 – 607, 1929.

[15]The *type* of a tetrahedron is just the radii of spheres centered in its vertices, there are 5 types: $1111, 111r, 11rr, 1rrr$, and $rrrr$.

[Bli69] G. Blind. Über Unterdeckungen der Ebene durch Kreise. *Journal für die Reine Angewandte Mathematik*, pages 145–173, 1969.

[CCMFT23] C. Chinaud-Chaix, N. Marchenko, T. Fernique, and S. Tricard. Do chemists control plane packing, i.e. two-dimensional self-assembly, at all scales? *New Journal of Chemistry*, 47(15):7014–7025, April 2023. Publisher: The Royal Society of Chemistry.

[CE03] H. Cohn and N. Elkies. New upper bounds on sphere packings I. *Annals of Mathematics*, 157(2):689–714, 2003.

[CG21] R. Connelly and S. J. Gortler. Packing disks by flipping and flowing. *Discrete & Computational Geometry*, 66:1262–1285, 2021.

[CGSY18] R. Connelly, S. Gortler, E. Solomonides, and M. Yampolskaya. Circle packings, triangulations, and rigidity. *Oral presentation at the conference for the 60th birthday of Thomas C. Hales*, 2018.

[CKM+17] H. Cohn, A. Kumar, S. Miller, D. Radchenko, and M. Viazovska. The sphere packing problem in dimension 24. *Annals of Mathematics*, 185(3), 2017.

[CW10] H. Chang and L. Wang. A simple proof of thue's theorem on circle packing. *https://arxiv.org/abs/1009.4322*, 2010.

[Del34] B. Delaunay. Sur la sphere vide. *Izv. Akad. Nauk SSSR, Otdelenie Matematicheskii i Estestvennyka Nauk*, 7(793-800):1–2, 1934.

[dGPW90] C. de Groot, R. Peikert, and D. Würtz. The optimal packing of ten equal circles in a square. *IPS Research Report*, 90-12, 01 1990.

[DLDOFV14] D. De Laat, F. M. De Oliveira Filho, and F. Vallentin. Upper bounds for packings of spheres of several radii. *Forum of Mathematics, Sigma*, 2:e23, 2014.

[Fer21] T. Fernique. Compact packings of space with two sizes of spheres. *Discrete & Computational Geometry*, 65(4):1287–1295, 2021.

[Fer22] T. Fernique. Density of binary disc packings: Lower and upper bounds. *Experimental Mathematics*, pages 1–12, 2022.

[FHS21] T. Fernique, A. Hashemi, and O. Sizova. Compact packings of the plane with three sizes of discs. *Discrete & Computational Geometry*, 66(2):613–635, 2021.

[Flo60] A. Florian. Ausfüllung der Ebene durch Kreise. *Rendiconti del Circolo Matematico di Palermo*, 9:300–312, 1960.

[Fod99] F. Fodor. The densest packing of 19 congruent circles in a circle. *Geometriae Dedicata*, 74(2):139–145, 1999.

[Fod00] F. Fodor. The densest packing of 12 congruent circles in a circle. *Beiträge zur Algebra und Geometrie*, 41(2):401–409, 2000.

[Fod03] F. Fodor. The densest packing of 13 congruent circles in a circle. *Beiträge zur Algebra und Geometrie*, 44, 2003.

[FP23] T. Fernique and D. Pchelina. Density of triangulated ternary disc packings. *Computational Geometry*, 115:102032, 2023.

[FP25] T. Fernique and D. Pchelina. Bounding the density of binary sphere packing. *https://arxiv.org/abs/2505.14110*, 2025.

[FT42] L. Fejes Tóth. Über die dichteste Kugellagerung. *Math. Z.*, 48:676–684, 1942.

[FT53] L. Fejes Tóth. *Lagerungen in der Ebene, auf der Kugel und im Raum*. Springer, Berlin, Heidelberg, 1953.

[FT64] L. Fejes Tóth. *Regular Figures*, volume 48 of *International Series of Monographs on Pure and Applied Mathematics*. Macmillan, 1st edition, 1964.

[FT84] L. Fejes Tóth. Compact packing of circles. *Studia Sci. Math. Hungar.*, 19:103–107, 1984.

[FTM58] L. Fejes Tóth and J. Molnár. Unterdeckung und Überdeckung der Ebene durch Kreise. *Mathematische Nachrichten*, 18:235–243, 1958.

[Gau31] C. F. Gauss. Untersuchungen über die Eigenschaften der positiven ternären quadratischen Formen von Ludwig August Seber. *Göttingische gelehrte Anzeigen*, 1831.

[GO04] J. E. Goodman and J. O'Rourke, editors. *Handbook of Discrete and Computational Geometry, Second Edition*. Chapman and Hall/CRC, Boca Raton, 2nd edition edition, 2004.

[HAB+17] T. C. Hales, M. Adams, G. Bauer, D. T. Dang, J. Harrison, T. L. Hoang, C. Kaliszyk, V. Magron, S. McLaughlin, T. T. Nguyen, T. Q. Nguyen, T. Nipkow, S. Obua, J. Pleso, J. Rute, A. Solovyev, A. H. T. Ta, T. N. Tran, D. T. Trieu, J. Urban, K. K. Vu, and R. Zumkeller. A formal proof of the Kepler conjecture. *Forum of Mathematics, Pi*, 5:e2, 2017.

[Hal92] T. C. Hales. The sphere packing problem. *Journal of Computational and Applied Math*, 44:41–76, 1992.

[Hal93] T. C. Hales. Remarks on the density of sphere packings in three dimensions. *Combinatorica*, 13(2):181–197, 1993.

[Hal05] T. C. Hales. A proof of the Kepler conjecture. *Annals of Mathematics*, 162(3):1065–1185, 2005.

[Hep00] A. Heppes. On the densest packing of discs of radius 1 and $\sqrt{2}-1$. *Studia Scientiarum Mathematicarum Hungarica*, 36:433–454, 2000.

[Hep03] A. Heppes. Some densest two-size disc packings in the plane. *Discrete & Computational Geometry*, 30:241–262, 2003.

[HF06] T. C. Hales and S. P. Ferguson. The Kepler conjecture. *Discrete & Computational Geometry*, 36(1):1–269, 2006.

[Hil02] D. Hilbert. Mathematical problems. *Bulletin of the American Mathematical Society*, 8(10):437 – 479, 1902.

[HST12] A. B. Hopkins, F. H. Stillinger, and S. Torquato. Densest binary sphere packings. *Phys. Rev. E*, 85:021130, 2012.

[Ken05] T. Kennedy. A densest compact planar packing with two sizes of discs. https://arxiv.org/abs/math/0412418, 2005.

[Ken06] T. Kennedy. Compact packings of the plane with two sizes of discs. *Discrete & Computational Geometry*, 35(2):255–267, 2006.

[Kep11] J Kepler. *Strena Seu de Niue Sexangula*. 1611. Translated by Hardie, C. in J. Kepler, *The Six-Cornered Snowflake*, Oxford University Press, 1966.

[KM23] E. Kikianty and M. Messerschmidt. On compact packings of Euclidean space with spheres of finitely many sizes. https://arxiv.org/abs/2305.00758, 2023.

[KMP+08] L. Kettner, K. Mehlhorn, S. Pion, S. Schirra, and C. Yap. Classroom examples of robustness problems in geometric computations. *Comput. Geom.*, 40:61–78, 01 2008.

[KW87] K. Kirchner and G. Wengerodt. Die dichteste packung von 36 kreisen in einem quadrat. *Beiträge zur Algebra und Geometrie*, 25:147–159, 1987.

[LS90] B. D. Lubachevsky and F. H. Stillinger. Geometric properties of random disk packings. *Journal of Statistical Physics*, 60(5):561–583, September 1990.

[Mar07] M. Markot. Interval methods for verifying structural optimality of circle packing configurations in the unit square. *Journal of Computational and Applied Mathematics - J COMPUT APPL MATH*, 199, 02 2007.

[Mar21] M. C. Markót. Improved interval methods for solving circle packing problems in the unit square. *Journal of Global Optimization*, 81(3):773–803, 2021.

[Mel94] H. Melissen. Densest packings of eleven congruent circles in a circle. *Geometriae Dedicata*, 50(1):15–25, 1994.

[Mes23] M. Messerschmidt. The number of configurations of radii that can occur in compact packings of the plane with discs of n sizes is finite. *Discrete & Computational Geometry*, 2023.

[MSS22] A. Mazel, I. Stuhl, and Y. Suhov. Minimal area of a voronoi cell in a packing of unit circles, 2022.

[Mud93] D. J. Muder. A new bound on the local density of sphere packings. *Discrete & Computational Geometry*, 10(4):351–375, 1993.

[NO99] K. J. Nurmela and P. R. J. Ostergård. More optimal packings of equal circles in a square. *Discrete & Computational Geometry*, 22(3):439–457, 1999.

[PDKM15] T. Paik, B. T. Diroll, C. R. Kagan, and C. B. Murray. Binary and ternary superlattices self-assembled from colloidal nanodisks and nanorods. *Journal of the American Chemical Society*, 137(20):6662–6669, 2015.

[Pir69] U. Pirl. Der Mindestabstand von n in der Einheitskreisscheibe gelegenen Punkten. *Mathematische Nachrichten*, 40:111–124, 1969.

[PWMdG92] R. Peikert, D. Würtz, M. Monagan, and C. de Groot. Packing circles in a square: A review and new results. *System Modelling and Optimization, Proceedings of the Fifteenth IFIP Conference*, 180:45–52, 1992.

[Rog58] C. A. Rogers. The packing of equal spheres. *Proceedings of the London Mathematical Society*, s3-8(4):609–620, 1958.

[Sch70] B. L. Schwartz. Separating points in a rectangle. *Journal of Recreational Mathematics*, 3(4):195–204, 1970.

[Sei40] F. Seitz. *The Modern Theory Of Solids*. International Series in Physics. New York McGraw-Hill Book Co., Inc., 1940.

[SM65] J. Schaer and A. Meir. On a geometric extremum problem. *Canadian Mathematical Bulletin*, 8(1):21–27, 1965.

[SMC+07] P. Szabó, M. Markot, T. Csendes, E. Specht, L. G. Casado, and I. García Fernandez. *New Approaches to Circle Packing in a Square: With Program Codes*. 01 2007.

[Spe25] E. Specht. *http://www.packomania.com*, 2025.

[Szp03] G. G. Szpiro. *Kepler's Conjecture: How Some of the Greatest Minds in History Helped Solve One of the Oldest Math Problems in the World*. Wiley, 2003.

[Thu10] A. Thue. Über die dichteste Zusammenstellung von kongruenten Kreisen in einer Ebene. *Christiania Videnskabs-Selskabets Skrifter*, I. Math.-Naturv. Klasse, 1:1–9, 1910.

[Via17] M. Viazovska. The sphere packing problem in dimension 8. *Annals of Mathematics*, 185(3), 2017.

[Wen83] G. Wengerodt. Die dichteste packung von 16 kreisen in einem quadrat. *Beiträge zur Algebra und Geometrie*, 16:173–190, 1983.

[Wen87a] G. Wengerodt. Die dichteste packung von 14 kreisen in einem quadrat. *Beiträge zur Algebra und Geometrie*, 25:25–46, 1987.

[Wen87b] G. Wengerodt. Die dichteste packung von 25 kreisen in einem quadrat. *Annales Universitatis Scientiarum Budapestiensis. Eötvös Sectio Mathematica*, 30:3–15, 1987.

Daria Pchelina
CNRS, France
LIP, ENS de Lyon, Lyon, France
Email: daria.pchelina@ens-lyon.fr